ACS Catalysis

Research Article

pubs.acs.org/acscatalysis

Formation, Operation and Deactivation of Cr Catalysts in Ethylene Tetramerization Directly Assessed by Operando EPR and XAS

Jabor Rabeah, Matthias Bauer,[†] Wolfgang Baumann, Ann E. C. McConnell,[#] William F. Gabrielli,[‡] Paul B. Webb,[‡] Detlef Selent, and Angelika Brückner*

Leibniz-Institut für Katalyse an der Universität Rostock, Albert-Einstein-Strasse 29a, D-18059 Rostock, Germany

Supporting Information

ABSTRACT: Operando EPR under elevated ethylene pressure supported by in situ XAS was for the first time applied to discriminate between active and deactivating Cr species in ethylene tetramerization. Starting from Cr(III) in the $Cr(acac)_3$ precursor, a (PNP)Cr(II)-$(CH_3)_2$ complex is most likely formed upon adding PNP and MMAO, which is regarded as the active species that converts ethylene to 1-octene by passing a reversible redox cycle, while reduction to Cr(I) leads to deactivation.

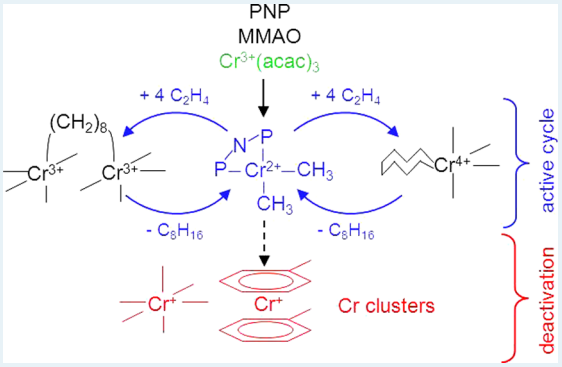

KEYWORDS: *chromium complexes, ethylene tetramerization, homogeneous catalysis, operando EPR, reaction mechanisms*

INTRODUCTION

Linear α-olefins, such as 1-hexene and 1-octene, are important building blocks for polymer production. They are generally produced by metal-catalyzed oligomerization of ethylene which, however, suffers from low selectivity, leading to a wide distribution of chain lengths. A breakthrough in ethylene tetramerization was achieved using Cr complexes with bidentate diphosphinoamine (PNP) ligands activated by modified methylaluminoxane (MMAO).[1] Since this time, many efforts have been made to further optimize their catalytic performance.[2,3] A chromacycle mechanism including oxidative coupling of C_2H_4 to Cr followed by further insertion of C_2H_4 into the Cr−C bond and final reductive elimination of 1-octene has been evidenced;[4,5] however, the structure and valence state of the active Cr species is still not clear. Single Cr sites cycling between Cr(II)/Cr(IV)[6,7] and Cr(I)/Cr(III)[8−10] oxidation states during reaction have been proposed for different catalysts. Recently, even a C_8-bridged Cr dimer, stabilized by PNP bridges has been proposed as the active site for ethylene tetramerization (although without specifying the Cr valence state), since the formation of a mononuclear chromacyclononane intermediate was considered as energetically improbable.[11] Our previous in situ EPR studies of $Cr(acac)_3$/PNP/MMAO solutions under static ethylene pressure suggested that single Cr(I) sites may not be the major active species and that coordination of PNP prevents deep reduction of Cr(III) to Cr(I) which was much more pronounced in $Cr(acac)_3$/MMAO solutions without PNP.[12] However, these earlier experiments suffered from the fact that intimate mixing of ethylene with the catalyst solution was not possible, which might have hindered the reaction.[12]

In this work, we present for the first time true operando EPR measurements of monovalent Cr(I) in Cr/PNP/MMAO solutions at 40 °C under flowing ethylene up to 14 bar. The effect of total pressure as well as the influence of different solvents, such as cyclohexane (CH), toluene (TOL), chloro- and fluorobenzene (CBz, FBz), has been analyzed and correlated with catalytic activity. To check for the presence of EPR-silent Cr(II), XANES/EXAFS measurements were performed.

EXPERIMENTAL SECTION

Materials. $Ph_2PN(^iPr)PPh_2$ (PNP), the structure of which is depicted in the Supporting Information (SI, Scheme SI-1) was prepared as described elsewhere.[1] MMAO-3A (7 wt % Al in heptane) was obtained from AkzoNobel. All manipulations were performed in the absence of moisture and air in a glovebox, and predried solvents were used. Solutions of 1.25 mM $Cr(acac)_3$/PNP were prepared in a glovebox by dissolving 8.74 mg of $Cr(acac)_3$ and 10.64 mg of the PNP ligand in 20 mL of dry solvent, that is, cyclohexane (CH, Aldrich), toluene (Tol, Aldrich), chlorobenzene (CBz, Aldrich), or fluorobenzene (FBz, Fluka).

Operando EPR Measurements. A special thick-wall quartz EPR tube reactor has been built and connected to a

Received: June 14, 2012
Revised: November 30, 2012
Published: December 3, 2012

gas circulation system (Warnow Hydraulik) containing an ethylene reservoir from which ethylene was continuously bubbled via a capillary into the reaction solution at different ethylene pressures (Supporting Information Figure SI-1). The reactor tube was implemented in the cavity of a cw-EPR spectrometer (ELEXSYS 500-10/12, Bruker). EPR spectra were recorded at 40 °C with a microwave power of 6.3 mW, a modulation frequency of 100 kHz, and modulation amplitude of 1 or 5 G. The tube was three times evacuated for 15 min to 10^{-4} mbar and subsequently filled with argon passed through an oxygen trap cartridge. After the third evacuation, the system was filled with ethylene, and solutions of MMAO-3A and Cr-ac/PNP were subsequently quickly injected into the EPR tube via a syringe under ethylene flow at normal pressure. The system was then closed, the ethylene pressure was raised to the desired value, and EPR spectra were recorded as a function of time during bubbling of ethylene. For comparison, blind experiments without bubbling of ethylene through the reaction mixture were also performed at 40 °C.

The Cr(I) concentrations in selected samples were determined by comparing the EPR signal areas (double integrals) of Cr(I) with that of a 2.6×10^{-4} M solution of DPPH in cyclohexane. For these measurements, a rectangular double cavity (Bruker) was used.

At the end of each experiment, excess ethylene was vented after cooling the EPR cell to room temperature. The volume of the liquid inside the cell was measured, and the reaction mixture was transferred to a GC vial. Two drops of a 10% aqueous HCl solution were added to the GC vial by a Pasteur pipet, and the solution was well mixed. After separation of the aqueous and the organic layers, 1 μL of the organic layer was injected into the GC (class 17C Shimadzu), and the product mixture was quantitatively analyzed for 1-octene and 1-hexene using a HP-PONA capillary column (Agilent 1909).

Computer simulation of Cr(I) EPR spectra was performed by the program SimFonia[13] using the spin Hamiltonian (eq 1),

$$H = \mu_B SgB_0 + SAI \tag{1}$$

in which μ_B is the Bohr magneton, S is the electron spin operator, g is the g tensor, B_0 is the magnetic field vector, A is the hyperfine coupling tensor, and I is the nuclear spin operator.

In Situ EXAFS and XANES Measurements. X-ray absorption measurements were performed at the XAS beamline at the Ångströmquelle Karlsruhe (ANKA). The synchrotron beam current was between 80 and 140 mA at 2.5 GeV storage ring energy. A Si(111) double crystal monochromator was used for measurements at the Cr K edge (5989 eV). The second monochromator crystal was tilted for optimal harmonic rejection. To perform in situ studies, the spectra were recorded in fluorescence mode using a hyperpure germanium detector. Energy calibration was performed with a chromium metal foil simultaneous to the reference measurements and prior to the measurements in solution.

The solid state reference samples were prepared under Ar atmosphere in a glovebox. They were embedded in a degassed polyethylene matrix and pressed into a pellet, which was sealed. For air- and moisture-sensitive samples, liquid samples were measured in a specially designed transmission sample cell that is equipped with tabs to be connected to a Schlenk line. The cell can be evacuated under elevated temperature and flushed with argon prior to the measurements. Air-sensitive samples can be filled in with syringes under inert conditions.

In situ studies were carried out with a setup described elsewhere.[14] Liquid samples were prepared from a solution of $Cr(acac)_3$ (2.0 mM) in freshly distilled cyclohexane and toluene. The PNP ligand was added in a first step in a molar ratio of 1:1. In a second step, MMAO was added in a 1:100 molar ratio to the solution in cyclohexane. The solutions were allowed to equilibrate for 10 min prior to the measurements. Five to ten scans were averaged to achieve a good signal-to-noise ratio. Thus, each spectrum took 30 min. For the measurement of $Cr(acac)_3$/MMAO in the absence of the PNP ligand, the same excess of MMAO was used.

For the XANES analysis, all spectra were carefully calibrated in energy. Then pre-edge and edge contributions according to the method described by Tromp et al. were identified.[15] To determine the smooth part of the EXAFS spectra, corrected for pre-edge absorption, a piecewise polynomial was used. It was adjusted in such a way that the low-R components of the resulting Fourier transform were minimal. After division of the background−subtracted spectrum by its smooth part, the photon energy was converted to photoelectron wave numbers k. The resulting $\chi(k)$ function was weighted with k^3. Single scattering data analysis was performed in k space according to the curved wave formalism of the EXCURV98 program with XALPHA phase and amplitude functions.[16] Multiple scattering calculations were not carried out because this would require exact knowledge about the structures formed in solution. The mean free path of the scattered electrons was calculated from the imaginary part of the potential (VPI set to −4.00). An overall amplitude reduction factor (AFAC) was adjusted to 0.8 using the known solid state structure of $Cr(acac)_3$. Fourier filtered spectra were analyzed in a k interval of $\Delta k = 8$ Å^{-1} (3−11) to separate random noise. The filtered interval in r space was $\Delta r = 3$ Å. According to the Nyqvist criterion, this resulted in $N_i = 2\Delta r \Delta k/\pi + 2 = 17$ free parameters in the fitting procedure, allowing for at least four shells with three paramters each to be adjusted. The quality of fit is given in terms of the R factor[17] according to eq 2.

$$R = \sum_i \frac{k^3|\chi^{exp}(k_i) - \chi^{theo}(k_i)|}{k^3|\chi^{exp}(k_i)|} \times 100\% \tag{2}$$

Comparison of two fitting models applied to one and the same experimental data is achieved by the reduced χ^2 (eq 3), which is an absolute index of the quality of the fit, taking into account the degree of overdeterminacy of the system and, therefore, allows direct comparison of different models with varying numbers of fitted parameters.[18]

$$\chi^2 = \frac{N_i/N}{N_i - p} \sum_i \frac{1}{\sigma_i^2}(\chi^{exp}(k_i) - \chi^{theo}(k_i))^2 \tag{3}$$

In eq 3, N is the number of data points, p is the number of fitted parameters and N_i is the number of independent degrees of freedom in the data according to the Nyqvist equation above. The statistical parameter σ_i used in χ^2 is given by eq 4.

$$\frac{1}{\sigma_i} = \frac{k_i^n}{\sum_j k_j^n |\chi_j^{exp}(k_j)|} \tag{4}$$

RESULTS AND DISCUSSION

Operando EPR Study. In the EPR spectra of $Cr(acac)_3$/PNP solutions in CH, two signals of low-spin Cr(I) species (S = 1/2) appear with time after adding MMAO (Figure 1),

dx.doi.org/10.1021/cs300686m | ACS Catal. 2013, 3, 95−102

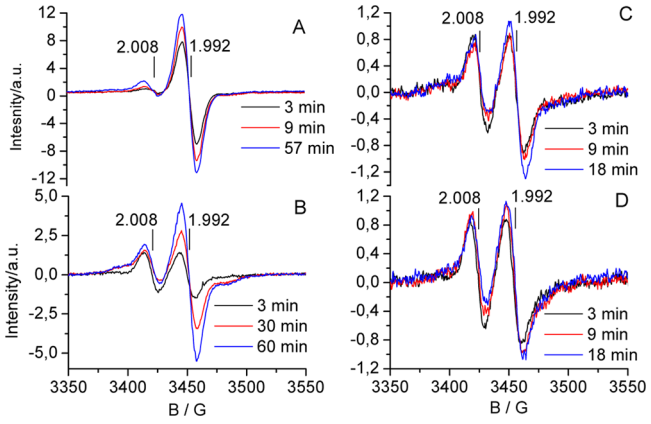

Figure 1. EPR spectra of Cr-ac/PNP/MMAO in cyclohexane at 40 °C recorded at different reaction times (A) without pressurizing the reactor with C_2H_4 (blind experiment) and during bubbling of ethylene at different pressures: $p(C_2H_4)$ = (B) 5, (C) 10, and (D) 14 bar.

indicating that MMAO reduces Cr(III), in agreement with previous results.[9,11,12] These signals have been assigned to Cr(I) complexes with (g = 2.008) and without a coordinated PNP ligand (g = 1.992).[12] Interestingly, the percentage of Cr(I) with respect to the total Cr content amounts to only 9.8% when no ethylene is added to the system and decreases even more strongly when ethylene is bubbled through the solution, amounting to only 1.9% Cr(I) at 14 bar C_2H_4 after 18 min of reaction time (Figure 1, Table 1).

In a previous in situ EPR study, we found that the Cr(III) signal of $Cr(acac)_3$ disappears completely within a few minutes after adding MMAO to the $Cr(acac)_3$/PNP solution, and no other Cr(III) signal appears.[12] This excludes a monomer Cr(III) intermediate as a possible resting state. On the other hand, only a minor amount of the total Cr content in the solution is reflected by the Cr(I) signals in Figure 1. This suggests that the major amount of Cr in the solution, including the active species, is converted into EPR-silent species. One can think of two possibilities: (i) formation of antiferromagnetic dimers or clusters (or both) and (ii) formation of Cr(II) single sites. This aspect is discussed in more detail below.

The relative intensities of the EPR signals related to PNP-containing and PNP-free Cr(I) species have been estimated using the amplitude of the positive lobe of the line at g = 2.008 and the negative lobe of the signal at 1.992 (Figure 1) together with the values of the total Cr(I) content (Table 1, column 3–5). In the absence of ethylene, the percentage of PNP-containing Cr(I) species in the CH solution is markedly lower than that of the PNP-free Cr(I) complex and does not change very much with rising ethylene pressure. This line represents only a minor part of the Cr–PNP complexes in solution. On the other hand, since coordination of the PNP ligand to Cr is supposed to account for the preferential formation of 1-octene and 1-hexene[1] (also confirmed by the values in Table 1), the low intensity of the Cr(I)-PNP signals in Figure 1 suggests, in agreement with previous results,[12] that coordination of PNP partially prevents deep reduction to Cr(I) and renders Cr sites in an EPR-silent state as supported, too, by XAS results discussed below.

In contrast, the signal intensity of the Cr(I) complex not containing a PNP ligand (g = 1.992) decreases markedly with rising C_2H_4 pressure while catalytic activity rises (Table 1). A similar trend is also observed for CBz and FBz solutions (spectra not shown). This suggests that, similar to PNP, coordination of C_2H_4 to the Cr site, being essential for a properly working catalytic cycle, may prevent deep reduction to Cr(I). Consequently, this implies that EPR signals in Figure 1 do not reflect the site that is responsible for selective hexene/octene formation.

The time dependence of the total Cr(I) signal intensity was evaluated using first-order kinetics (eq 5), in which $[Cr_{prec}]$ denotes the molar fraction of the Cr precursor species from which EPR-visible Cr(I) is formed (Figure 2).

$$[Cr(I)] = [Cr_{prec}](1 - e^{-kt}) \quad (5)$$

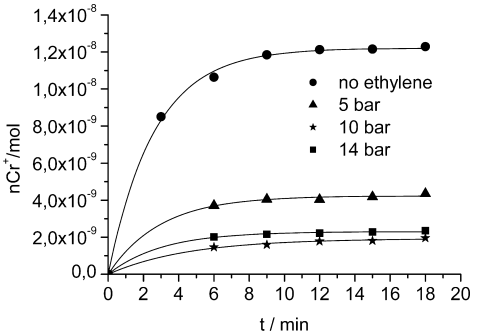

Figure 2. Amount of Cr(I) in the reactor (symbols) after different reaction times (derived from spectra in Figure 1) and kinetic fits using eq 5 (lines).

Table 1. Relative Cr(I) Percentage, Ethylene Consumption and Productivity of 1-C_8H_{16} and 1-C_6H_{12}[a] Measured after Different Reaction Times

solvent, $p_{C_2H_4}$ [bar]	reaction time [min]	Cr(I)/Cr_{total} [%]	PNP-Cr(I)[b]	Cr(I)[b]	consumption [$g_{C_2H_4}/g_{Cr}h$]	productivity [$g_{olefin}/g_{Cr}h$]
CH, 0	18	9.8	0.8	9.0		
CH, 5	60	7.2	1.9	5.3	800	32 (16)
CH, 10	18	1.6	0.6	1.0	7995	1780 (1020)
CH, 14	18	1.9	0.9	1.0	10660	3000 (1290)
tol, 0	36	99.3	4.8	94.5		
tol, 14	36	100.0		100	1333	21 (7)
CBz, 0	18	53.0	0.9	52.1		
CBz, 14	18	19.0	1.5	17.5	13326	3170 (2620)
FBz, 0	18	49.3	1.8	47.5		
FBz, 14	18	5.2	0.8	4.4	15991	4630 (2900)

[a]Values in parentheses. [b]These values indicate the relative percentage of PNP-bound Cr(I) (signal at g = 2.008 in Figure 1) and PNP-free Cr(I) (signal at g = 1.992 in Figure 1).

dx.doi.org/10.1021/cs300686m | ACS Catal. 2013, 3, 95–102

In CH, independent of the ethylene pressure, $[Cr_{prec}]$ values are markedly lower than the initial $Cr(acac)_3$ amount in the samples, which was always 1.25×10^{-7} mol (Table 2). This means that the Cr(I) species reflected by the EPR signals in Figure 1 are not directly formed from Cr(III) but, rather, from EPR-silent intermediates, possibly Cr(II). This agrees with previous in situ EPR results, which have shown that the decline of Cr(III) from $Cr(acac)_3$ by reduction with MMAO is much faster than the formation of Cr(I), suggesting that an EPR-silent intermediate is passed.[12]

Table 2. Results of Kinetic Fits Using Eq 5[a]

solvent, $p_{C_2H_4}$ [bar]	$[Cr_{prec}]$[b] [10^{-7} mol]	k [min^{-1}]
CH, 0	0.120	0.380
CH, 5	0.043	0.340
CH, 10	0.019	0.219
CH, 14	0.023	0.330
tol, 0	1.25	0.143
CBz, 0	0.81	0.098
FBz, 0	0.8	0.081

[a]Figure 2. [b]Initial concentration, $[Cr(acac)_3]_0 = 1.25 \times 10^{-7}$ mol in all samples

In toluene solution, $Cr(acac)_3$ is completely transformed to a PNP-free Cr(I) complex in the absence of ethylene,[12] and the same is observed at 14 bar C_2H_4 (Figure 3). At low modulation amplitude, superhyperfine splitting (shfs) from the coupling of the electron spin with the nuclear spin of 10 equivalent protons from two toluene molecules can be resolved, indicating the complete formation of a $[Cr(\eta^6\text{-}CH_3C_6H_5)_2]^+$ sandwich complex (inset in Figure 3). The isotropic values $g_{iso} = 1.991$ and $A_{iso} = 3.47$ G derived by spectra simulation (Supporting Information Figure SI-2A, Table SI-1) are in excellent agreement with values found for the $[Cr(\eta^6\text{-}CH_3C_6H_5)_2]^+$ cation in CH_3CN solution.[19]

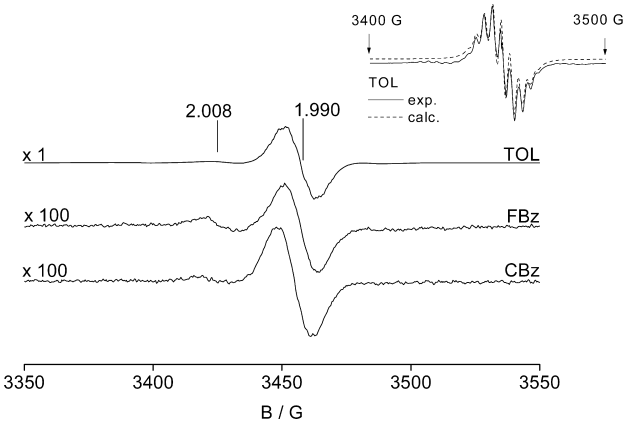

Figure 3. EPR spectra of Cr-ac/PNP/MMAO in different aromatic solvents at 40 °C under 14 bar C_2H_4. Inset shows spectrum in toluene measured at 1 G modulation amplitude showing shfs from 10 protons.

Interestingly, ethylene consumption and production rates of 1-hexene and 1-octene are about 1 order of magnitude lower than in CH under the same conditions (Table 1). This shows clearly that fast and complete encapsulation of the whole Cr within a $[Cr(\eta^6\text{-}CH_3C_6H_5)_2]^+$ sandwich complex, in which the PNP ligand is prevented from coordinating to Cr, is the main reason for the dramatic loss of activity. Kinetic evaluation of this process by eq 5 (Table 2) reveals that $[Cr_{prec}] = [Cr(III)]_0$; that is, that the initial Cr(III) from $Cr(acac)_3$ is directly transformed to the diarene sandwich complex without passing an EPR-silent intermediate.

The EPR signal detected at $g = 1.990$ in CBz and FBz at 40 °C under 14 bar C_2H_4 (Figure 3) also arises from the respective $[Cr(arene)_2]^+$ complexes, as confirmed by the spectra simulation shown in the Supporting Information, Figures SI-2b and SI-3. However, after 18 min, only about half of the total Cr in solution is sandwiched by CBz and FBz in the absence of C_2H_4, and this drops to <20% under 14 bar ethylene, in contrast to 100% in toluene (Table 1). Moreover, kinetic evaluation of the increase of the $[Cr(arene)_2]^+$ EPR signal with time by eq 5 reveals that $[Cr_{prec}]$ is 0.8×10^{-7} mol, markedly smaller than the initial $Cr(acac)_3$ amount in the sample (1.25×10^{-7} mol). This indicates that the $[Cr(arene)_2]^+$ complexes with CBz and FBz are not directly formed from initial Cr(III) but, rather, from an EPR-silent intermediate.

By comparing the values in Table 2, it is evident that, for a given solvent, increasing ethylene pressure suppresses formation of Cr(I) single sites, and this goes along with increasing catalytic activity, suggesting that the EPR-visible Cr(I) complexes are not the active species for ethylene tetramerization. Within the series of the monosubstituted benzenes, the trend to form catalytically inactive $[Cr(arene)_2]^+$ complexes decreases with the electron-withdrawing effect of the substituent in the order TOL ≫ CBz > FBz. In the same order, catalytic activity increases. Obviously, the lower the electron density of the aromatic π-system, the weaker its coordination to Cr and its ability to displace PNP and C_2H_4 from approaching the active Cr site and to prevent deep reduction to Cr(I). In CH, which does not possess an aromatic π-system, coordination to Cr should be weakest. Consequently, the Cr(I) percentage detected by EPR under 14 bar ethylene is lowest (Table 1), and one would expect the best catalytic performance in this case. However, the catalytic activity in CH is surprisingly somewhat lower than in CBz and FBz, suggesting that, with too weak solvent coordination, deactivation pathways other than $[Cr(arene)_2]^+$ formation might play a role. Possibly, initially active Cr species agglomerate when solvent stabilization is too weak.

In Situ EXAFS and XANES Measurements. Unfortunately, EPR cannot detect the entire possible Cr valence states at temperatures applied in this study. Configurations with an even number of single electrons, such as Cr(II) and Cr(IV), are detectable, if at all, only at very low temperature, usually below 77 K. Therefore, we applied X-ray absorption spectroscopy as another independent method to assess the Cr coordination and valence state. The spectra of solid $Cr(acac)_3$ as well as of solutions in CH of $Cr(acac)_3$ + MMAO with and without added PNP are shown in Figure 4, and Table 3 contains the numeric parameters obtained by fitting the experimental EXAFS spectra with theoretical models. The spectrum after adding PNP to the $Cr(acac)_3$ solution in the absence of MMAO was essentially the same as the spectrum of pure $Cr(acac)_3$ and is therefore not shown.

According to the crystal structure of $Cr(acac)_3$, a three-shell model consisting of one oxygen shell with six atoms at 1.96 Å and two carbon shells with six and four atoms at 2.91 and 3.19 Å, respectively, is necessary to fit this solid reference (Figure 4a). The addition of excess MMAO to the solution of $Cr(acac)_3$ in CH in the absence of PNP leads to marked changes, which are obvious in the experimental spectra (Figure

dx.doi.org/10.1021/cs300686m | ACS Catal. 2013, 3, 95−102

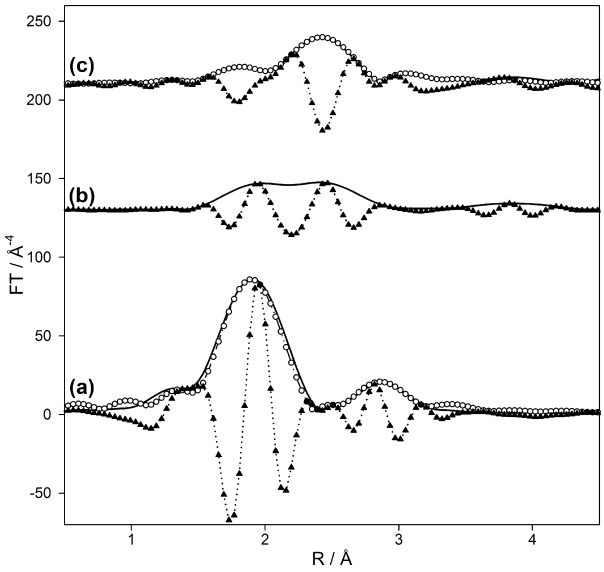

Figure 4. Experimental modulo (solid line) imaginary (dotted line, triangles) spectra together with the calculated modulo EXAFS function (dashed dotted line, circles) of (a) solid $Cr(acac)_3$ and solutions of (b) $Cr(acac)_3$ + MMAO in CH and (c) $Cr(acac)_3$ + PNP + MMAO in CH. Corresponding raw data are plotted in Supporting Information Figure SI-4.

4 b). As a result of the low signal-to-noise ratio, an EXAFS fitting result is not presented here because of the high uncertainty of the obtained parameters.

The spectrum changes again considerably by adding MMAO to a solution of $Cr(acac)_3$ and PNP in cyclohexane (Figure 4c). As can be seen in Table 3, only one light atom contribution remains at a distance higher than in $Cr(acac)_3$. It is generally assumed that the aluminoxane activator alkylates the metal center,[8,20,21] Therefore, this light atom shell is assigned to coordinating methyl groups. A similar Cr−C contribution at a distance of 2.06−2.11 Å was found by Evans et al. for related systems with sulfur-containing ligands.[22]

In their previous work, Evans et al. activated $CrCl_3$ with Me_3Al and found three methyl ligands coordinated per chromium center.[22] In contrast, in our work, the obtained Cr−C coordination number suggests only the coordination of two methyl groups (Table 3). An additional nearest neighbor shell containing 2.3 atoms at 2.42 Å could be unambiguously attributed to phosphorus of one coordinating PNP ligand. The determined Cr−P distance is similar to the Cr−S distance in Cr complexes with sulfur-containing ligands.[22] Consequently, the EXAFS results suggest the coordination of one PNP and two $[CH_3]^-$ ligands to the central Cr, thus forming a (PNP)Cr-(II)$(CH_3)_2$ complex. This implies that (i) that Cr(III) is reduced to Cr(II) upon addition of MMAO and (ii) direct coordination of PNP to Cr takes place only in the presence of MMAO.

It was not possible to fit a Cr−Cr shell in the range of 3−3.5 Å with statistical significance to the experimental spectrum in Figure 4d . Since two different models are compared (with and without Cr−Cr contribution), the reduced χ^2 has to be considered. Given the fact that a Cr−Cr shell resulted in χ^2 values of 136 (unfiltered data) and 31×10^{-6}, respectively, compared with 35 (unfiltered data) and 12×10^{-6} for the case without a Cr−Cr shell, this latter model is superior. Moreover, the Cr−Cr coordination number in the statistically inferior case was 0.2 ± 0.1, which supports the conclusion that such a pair is not formed when PNP is present in the solution before adding MMAO. This suggests that PNP stabilizes mononuclear Cr sites, thus preventing them from agglomeration, which could be a possible reason for deactivation.

It should be mentioned that the formation of a cationic $[(PNP)Cr(CH_3)]^+$ complex through alkyl abstraction by MMAO, which would lead to a Cr(III) center, seems highly improbable. This is supported by previous EPR measurements of the $Cr(acac)_3$/PNP/MMAO system, in which spectra were recorded after temporal quenching to 77 K to avoid too short Cr(III) relaxation times that could prevent the detection of Cr(III) at 20 °C.[12] In these studies, it was clearly shown that the Cr(III) signal is still properly seen right after adding MMAO to the $Cr(acac)_3$/PNP solution but vanishes with increasing reaction time. As mentioned above, there could be two reasons for the disappearance of the Cr(III) EPR signal: (i) agglomeration to antiferromagnetic Cr dimers or even polymers and (ii) reduction of Cr(III). On the basis of EXAFS data, a Cr−Cr interaction can be safely excluded for the $Cr(acac)_3$/PNP/MMAO system (Table 3). Therefore, reduction of Cr(III) and formation of a neutral (PNP)Cr(II)$(CH_3)_2$ species is most probable.

Although the EXAFS results strongly suggested an oxidation state of Cr(II) for the species formed from $Cr(acac)_3$ in cyclohexane with PNP and MMAO, a thorough XANES study was carried out to achieve further proof of this conclusion. As shown by different studies[22,23] the determination of the oxidation state of chromium complexes is not straightforward when different ligands, isomers, or coordination geometries are present. This can be seen from the XANES spectra of reference samples in Figure 5 and corresponding edge energies in Table 4 and also from XANES spectra of defined complexes of Cr(II) with different PNPs but the same number of two Cl ligands (Supporting Information Figure SI-5).

Table 3. Structural Parameters Obtained by Fitting the EXAFS Spectra in Figure 4 with Theoretical Models

sample	abs−bs[a]	N (bs)[b]	R (bs)[c]/Å	σ^d/Å^2	E_f^e/eV	R^f/%
solid $Cr(acac)_3$ (spectrum a)	Cr−O	*6*	1.96 ± 0.02	0.007 ± 0.001	5.25	12.9
	Cr−C	*6*	2.91 ± 0.03	0.009 ± 0.002		
	Cr−C	*3*	3.19 ± 0.03	0.009 ± 0.002		
$Cr(acac)_3$ + PNP + MMAO in CH (spectrum c)	Cr−C	1.5 ± 0.6	2.03 ± 0.02	0.002 ± 0.001	5.33	16.4
	Cr−P	2.3 ± 0.5	2.42 ± 0.02	0.009 ± 0.001		
	Cr−C	1.4 ± 0.5	2.78 ± 0.03	0.003 ± 0.001		

[a]Abs = X-ray absorbing atom, Bs = backscattering atom. [b]Number of neighbor backscattering atoms. [c]Distance between Abs and Bs. [d]Debye−Waller-like factor. Italic numbers indicate values that were fixed in the fitting process. [e]Shift between the experiment and the calculated EXAFS function. [f]Quality of fit.

dx.doi.org/10.1021/cs300686m | ACS Catal. 2013, 3, 95−102

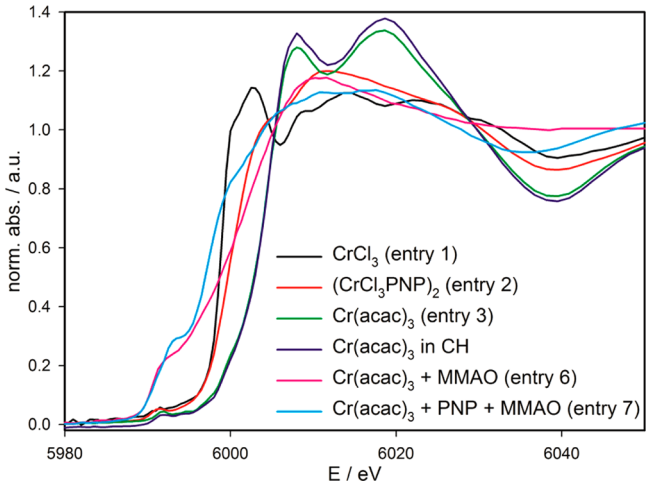

Figure 5. XANES spectra of the samples listed in Table 4.

The main edge energy of $CrCl_3$ and $Cr(acac)_3$ differs by 6.4 eV, although the coordination number and valence state are the same (Table 4). A difference of 2.1 eV appears when Cl in the coordination sphere of Cr is replaced by PNP (compare entries 1 and 2, Table 4). This shows that the exact oxidation state determination of structurally not well-defined species in the course of chemical reactions has thus to be considered with care. Nevertheless, we base our discussion here on the investigation of selected reference compounds in combination with previously published results[15] to derive empiric values on the influence of PNP ligands and coordination numbers on the edge position according to the procedure suggested by Tromp et al.[15]

To determine the oxidation state of Cr in the complex $(PNP)Cr(CH_3)_2$ formed upon adding MMAO to a solution of $Cr(acac)_3$ and PNP (entry 6 in Table 4), we use a XANES analysis of measurements presented in this study as well as in ref 15 to account for different oxidation states, coordination numbers, and the influence of the PNP ligand. In detail, the following procedure was applied: First, a possible shift in the main edge induced by coordinated PNP ligand was evaluated by comparison of the samples $CrCl_3$ (entry 1) and $(CrCl_3PNP)_2$ (entry 2). In comparison with the ligand-free $CrCl_3$, the PNP ligand causes a shift to higher edge energies of around 2.2 eV. Since the EXAFS analysis did not show any remaining acac ligand at the Cr ion in the sample $Cr(acac)_3$ + PNP + MMAO, the energy position of $Cr(acac)_3$ was not included in this discussion. Second, because the EXAFS analysis of $Cr(acac)_3$ + PNP + MMAO proved a coordination number of four, literature values (entry 4 and 5 in Table 4) were used to construct a "calibration" curve for such an environment. This was used as the upper limit for the oxidation state, and a second curve, shifted by 2.2 eV to account for the possible influence of the PNP ligand, marks the lower limit. This is shown in Figure 6.

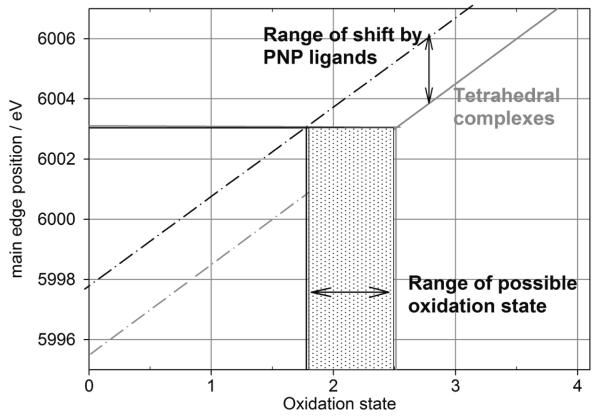

Figure 6. Oxidation state analysis by means of the main XANES feature. Details of the procedure are given in the text.

Within these two calibration curves, the edge position of 6003.2 eV for $Cr(acac)_3$ + PNP + MMAO is interpreted by a Cr oxidation state of 2.1+. This is in agreement with the oxidation state deduced from the EXAFS results by taking into account the coordinating ligands and the requirement of electroneutrality. Although this argumentation has to be considered rather crude, it is supported by comparison with literature on heterogeneous catalysts and minerals. Even if the XANES spectrum of $Cr(acac)_3$ + PNP + MMAO is lacking an intense prepeak, which would be characteristic of a low-symmetry environment, comparison with the work of Weckhuysen et al.[24] supports our assignment of both coordination number and oxidation state. In their work, a very similar XANES structure with a shoulder instead of a prepeak was found for a Cr(II) species coordinated by three nearest neighbors. This shoulder is caused by a 1s → 4s transition in low-symmetry environments.[25] Since according to the available literature, this shoulder is a unique feature of Cr(II) in a coordination of low symmetry,[24,25] the XANES analysis supports the conclusions from EPR results. Further support is provided by the XANES spectrum of $Cr(acac)_3$ after MMAO addition without PNP. In this case also, a prepeak characteristic of Cr(II) is detected, and the determined edge position is similar to the one found with PNP. The influence of the coordinated PNP ligand as already detected by comparison of entries 1 and 2 in Table 4 is also clearly visible in a broadened XANES spectrum. Finally, it must be mentioned

Table 4. Main Edge Positions Derived from the XANES Spectra in Figure 5[a] and from Ref 15[b]

no.	sample	oxidation state	Cr coordination number	main edge eV
1	$CrCl_3$	3+	6	5999.0
2	$(CrCl_3PNP)_2$	3+	6	6001.2
3	$Cr(acac)_3$	3+	6	6005.5
4	$CrCl_2(THF)_2$	2+	4	6001.5
5	$Cr(CH_3Si(CH_3)_3)_4$	4+	4	6007.5
7	$Cr(acac)_3$ + MMAO	(2.0 ± 0.4)+	EXAFS: 4–6	6002.1 (PP: 5991)
7	$Cr(acac)_3$ + PNP + MMAO	(2.1 ± 0.4)+	EXAFS: 4	6003.2 (PP: 5990.6)

[a]Entries 1–3, 6. [b]Entries 4, 5.

dx.doi.org/10.1021/cs300686m | ACS Catal. 2013, 3, 95–102

that in both cases, with and without PNP, certain fractions of Cr(I) are surely present, as deduced from the EPR results. However, since these contributions amount to a maximum of only 10%, they cannot be separated from the major Cr(II) part due to the low overall chromium concentration.

Proposed Reaction Mechanism. On the basis of the integrated evaluation of operando EPR and in situ XAS results, a possible reaction pathway can be proposed (Scheme 1). As

Scheme 1. Proposed Reaction Pathway Based on Operando EPR and X-ray Absorption Results

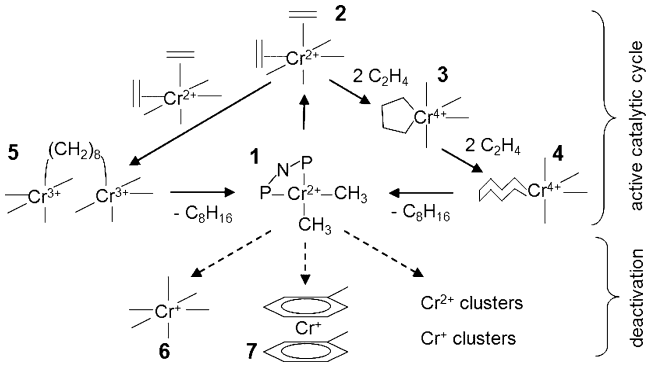

evidenced by EPR, interaction with MMAO and PNP leads to complete reduction of $Cr(acac)_3$. This has been clearly shown in our previous work by in situ EPR measurements at 77 K, which revealed a fast decline of the Cr(III) signal in a solution of $Cr(acac)_3$ and PNP in CH after addition of MMAO.[12] However, only a minor part of Cr reappears as Cr(I) in the EPR spectrum (Figure 1, Table 1). The acac ligands may be replaced by PNP and two methyl ligands, probably leading to a four-coordinated neutral $(PNP)Cr(II)(CH_3)_2$ intermediate **1** (suggested by EXAFS/XANES), which must contain divalent Cr to ensure electroneutrality. A cationic $[(PNP)Cr(III)(CH_3)_2]^+$ intermediate seems less probable, since pronounced reduction of Cr(III) was found previously[12,26] and other possible reasons that could hide Cr(III) from detection by EPR could be ruled out. This explains why the major part of the Cr in the sample is not seen by EPR under the applied conditions, since it might be divalent.

Intermediate **1** should have free coordination sites to interact with C_2H_4 and form intermediate **2**, in which the Cr oxidation state is still preserved. It is anticipated that the PNP and alkyl ligands remain attached to the Cr ion in the catalytic working state. However, for clear experimental evidence, in situ EXAFS measurements in the presence of ethylene are required, which are planned for the future. Oxidative addition of coordinated ethylene may lead to either a C_8-bridged dimer **5**, as proposed by S. Peitz et al.,[11] or to a chromacyclononane intermediate **4**, as proposed by others.[6,7] With the dimer **5**, a catalytic redox cycle involving a Cr(II)/Cr(III) pair should be passed, whereas a Cr(II)/Cr(IV) redox couple might be operative if a chromacyclononane intermediate **4** is formed. None of these Cr valence states is visible by EPR at the reaction temperature of 40 °C.[12] In both cases, reductive elimination of 1-octene would restore the tentative active Cr(II) species **1**.

In the absence of C_2H_4 or at too low C_2H_4 concentrations, the active complex **1** might alleviate unsaturation by coordinating solvent or MMAO molecules (or both). In turn, it may be further reduced to Cr(I) (species **6** and **7**, detected by EPR) or form clusters. These, however, might form only at extended reaction times, since EXAFS revealed no indication for the presence of closely neighboring Cr atoms after 30 min. Cr−Cr distances in dimers with a direct Cr−Cr bond were found to be around 1.8 Å,[27] whereas for a Cl-bridged $[(PNP)Cr(III)Cl_2(\mu\text{-}Cl)]_2$ complex, the Cr−Cr distance is 3.61 Å.[1] No Cr shell could be detected by EXAFS at a similar distance in the presence of PNP. However, it was found when no PNP is present in the system, suggesting that PNP plays a crucial role in stabilizing the active mononuclear Cr complex.

The extent of the pathway in Scheme 1 is widely dominated by the solvent properties. In toluene, solvent coordination is so effective that even at 14 bar ethylene, the deactivation route to the Cr(I) sandwich complex **7** dominates almost completely over the active cycle, and the intermediate **1** might have a negligible lifetime, as suggested by the kinetic results in Table 2. In weaker coordinating aromatic solvents CBz and FBz, the active cycle is favored over the deactivation route. Formation of **7** is markedly slower than in toluene. The lower olefin productivity in CH (Table 1) suggests that the deactivation should be more pronounced, as in CBz and FBz; however, the Cr(I) concentration detected by EPR is lower than in the latter two cases. This may be due to the fact that CH cannot stabilize single Cr(I) sites by forming a sandwich complex **7**. Possibly, species **6** tends to form clusters that, because of antiferromagnetic coupling, are not visible by EPR.

CONCLUSIONS

In summary, we have for the first time monitored Cr-catalyzed ethylene tetramerization by operando EPR under pressure. These EPR data, together with in situ XAS results support the conclusion that the tentative active species, which forms in situ from $Cr(acac)_3$ and PNP upon adding MMAO, is a $(PNP)Cr(II)(CH_3)_2$ complex. Depending on the mode of C_2H_4 coordination (chromacyclononane[6,7] or Cr−C_8H_{16}−Cr dimer[11]), it should pass either a Cr(II)/Cr(IV) or a Cr(II)/Cr(III) redox cycle. Deeper reduction to Cr(I) is a reason for deactivation.

Particular benefits arise from the combination of EPR and XAS spectroscopy because of their different selectivities for the detection of Cr species in different valence states. Although EPR can detect Cr(I) and Cr(III) but not Cr(II), XAS can, in principle, visualize all valence states of Cr. However, it faces difficulties in discerning Cr species of different valence states or coordination environments that coexist in the reaction solution. With all the given caution, the integrated evaluation of operando EPR and XAS results provides arguments that a Cr(II)/Cr(IV) redox cycle may be most probable in ethylene tetramerization over Cr−PNP complex catalysts.

ASSOCIATED CONTENT

Supporting Information

EPR reactor scheme and EPR spectra simulations, EXAFS raw data and XANES of Cr(II)-PNP model complexes. This information is available free of charge via the Internet at http://pubs.acs.org.

AUTHOR INFORMATION

Corresponding Author

*Phone: (+49) 381 1281 244. Fax: (+49) 381 1281 51 244. E-mail:angelika.brueckner@catalysis.de.

Present Addresses

[†]TU Kaiserslautern, Fachbereich Chemie, Erwin-Schrödinger-Str., Gebäude 45, D-66763 Kaiserslautern, Germany.
[#]Sasol Technology R&D, 1 Klazie Havenga Road, PO Box 11947, Sasolburg, South Africa.
[‡]Sasol Technology UK Ltd., Purdie Building, North Haugh, St. Andrews, FIFE, KY16 9ST, UK.

Notes

The authors declare no competing financial interest.

■ ACKNOWLEDGMENTS

ANKA (Karlsruhe) is acknowledged for provision of beamtime, and we thank Dr. Stefan Mangold for help and support during the measurements. M.B. acknowledges funding from the Carl-Zeiss foundation in frame of the junior professorship "Analytics of Catalytic Active Materials".

■ REFERENCES

(1) Bollmann, A.; Blann, K.; Dixon, J. T.; Hess, F. M.; Killian, E.; Maumela, H.; McGuinnes, D. S.; Morgan, D. H.; Neveling, A.; Otto, S.; Overett, M.; Slawin, A. M. Z.; Wasserscheid, P.; Kuhlmann, S. *J. Am. Chem. Soc.* **2004**, *126*, 14712−14713.

(2) Blann, K.; Bollmann, A.; de Bod, H.; Dixon, J. T.; Killian, E.; Nongodlwana, P.; Maumela, M. C.; Maumela, H.; McConnell, A. E.; Morgan, D. H.; Overett, M. J.; Prétorius, M.; Kuhlmann, S.; Wasserscheid, P. *J. Catal.* **2007**, *249*, 244−249.

(3) Overett, M. J.; Blann, K.; Bollmann, A.; de Villiers, R.; Dixon, J. T.; Hess, F. M.; Killian, E.; Maumela, M. C.; Maumela, H.; McGuinness, D. S.; Morgan, D. H.; Rucklidge, A.; Slawin, A. M. Z. *J. Mol. Catal. A: Chem.* **2008**, *283*, 114−119.

(4) Agapie, T.; Schofer, S. J.; Labinger, J. A.; Bercaw, J. E. *J. Am. Chem. Soc.* **2004**, *126*, 1304−1305.

(5) Tomov, A. K.; Chirinos, J. J.; Jones, D. J.; Long, R. J.; Gibson, V. C. *J. Am. Chem. Soc.* **2005**, *127*, 10166−10167.

(6) Jabri, A.; Crewdson, P.; Gambarotta, S.; Kokobkov, I.; Duchateau, R. *Organometallics* **2006**, *25*, 715−718.

(7) McGuinness, D. S.; Brown, D. B.; Tooze, R. P.; Hess, F. M.; Dixon, J. T.; Slawin, A. M. Z. *Organometallics* **2006**, *25*, 3605−3610.

(8) Rucklidge, A. J.; McGuinnes, D. S.; Tooze, R. P.; Slawin, A. M. Z.; Pelletier, J. D. A.; Hanton, M. J.; Webb, P. B. *Organometallics* **2007**, *26*, 2782−2787.

(9) Skobelev, I. Y.; Panchenko, V. N.; Lyakin, O. Y.; Bryliakov, K. P.; Zakharov, V. A.; Talsi, E. P. *Organometallics* **2010**, *29*, 2943−2950.

(10) McDyre, L.; Carter, E.; Cavell, K. J.; Murphy, D. M.; Platts, J. A.; Sampford, K.; Ward, B. D.; Gabrielli, W. F.; Hanton, M. J.; Smith, D. M. *Organometallics* **2011**, *30*, 4505−4508.

(11) Peitz, S.; Aluri, B. R.; Peulecke, N.; Müller, B. H.; Wöhl, A.; Müller, W.; Al-Hazmi, M. H.; Mosa, F. M.; Rosenthal, U. *Chem.—Eur. J.* **2010**, *16*, 7610−7676 and references therein.

(12) Brückner, A.; Jabor, J. K.; McConnell, A. E. C.; Webb, P. B. *Organometallics* **2008**, *27*, 3849−3856.

(13) WINEPR-SimFonia (version 1.26), Bruker Analytik GmbH: Rheinstetten, 1997.

(14) Bauer, M.; Heusel, G.; Mangold, S.; Bertagnolli, H. *J. Synchrotron Radiat.* **2010**, *17*, 273. Bauer, M.; Gastl, Chr. *Phys. Chem. Chem. Phys.* **2010**, *12*, 5575−5584.

(15) Tromp, M.; Moulin, J.; Reid, G.; Evans, J. *AIP Conf. Proc.* **2006**, *882*, 699−701.

(16) Binsted, N.; Hasnain, S. S. *J. Synchrotron Radiat.* **1996**, *3*, 185−196.

(17) Binsted, N.; , *EXCURV98: CCLRC Daresbury Laboratory computer program, Manual 1998*; Mosselman, F., Ed.; 1998.

(18) Bauer, M.; Bertagnolli, H. *J. Phys. Chem. B* **2007**, *111*, 13756−13764.

(19) Angelescu, E.; Nicolau, C.; Simon, Z. *J. Am. Chem. Soc.* **1966**, *88* (17), 3910−3912.

(20) Dixon, T. J.; Green, M. J.; Hess, F. M.; Morgan, D. H. *J. Organomet. Chem.* **2004**, *689*, 3641−3668.

(21) van Rensburg, W. J.; van den Berg, J.-A.; Steynerg, P. J. *Organometallics* **2007**, *26*, 1000−1013.

(22) Moulin, J. O.; Evans, J.; McGuinness, D. S.; Reid, G.; Rucklidge, A. J.; Tooze, R. P.; Tromp, M. *Dalton Trans.* **2008**, 1177−1185.

(23) Engemann, C.; Hormes, J.; Longen, A.; Dötz, K. H. *Chem. Phys.* **1998**, *237*, 471−481.

(24) Weckhuysen, B. M.; Schoonheydt, R. A.; Jehng, J.-M.; Wachs, I. E.; Cho, S. J.; Ryoo, R.; Kijlstra, S.; Poels, E. *Faraday Trans.* **1995**, *91*, 3245−3253.

(25) Berry, A. J.; O'Neill, H. S. C. *Am. Mineral.* **2004**, *89*, 790−798.

(26) van Rensburg, W. J.; Grove, C.; Steynberg, J. P.; Stark, K. B.; Huyser, J. J.; Steynberg, P. J. *Organometallics* **2004**, *23*, 1207−1222.

(27) La Macchia, G.; Li Manni, G.; Todorova, T. K.; Brynda, M.; Aquilante, F.; Roos, B. O.; Gagliardi, L. *Inorg. Chem.* **2010**, *49*, 5216−5222.

■ NOTE ADDED AFTER ASAP PUBLICATION

This paper was published on the Web on December 19, 2012, with minor text errors. The corrected version was reposted on January 4, 2013.